We are IntechOpen, the world's leading publisher of Open Access books Built by scientists, for scientists

6,900
Open access books available

186,000
International authors and editors

200M
Downloads

Our authors are among the

154
Countries delivered to

TOP 1%
most cited scientists

12.2%
Contributors from top 500 universities

CLARIVATE ANALYTICS
BOOK CITATION INDEX
INDEXED

WEB OF SCIENCE™

Selection of our books indexed in the Book Citation Index
in Web of Science™ Core Collection (BKCI)

Interested in publishing with us?
Contact book.department@intechopen.com

Numbers displayed above are based on latest data collected.
For more information visit www.intechopen.com

Multiscale, Generalised Stochastic Solute Transport Model in One Dimension

6.1 Introduction

In Chapter 3 and 4, we have developed a stochastic solute transport model in 1-D without rosorting to simplifying Fickian assumptions, but by using the idea that the fluctuations in velocity are influenced by the nature of porous medium. We model these fluctuations through the velocity covariance kernel. We have also estimated the dispersivity by taking the realisations of the solution of the SSTM and using them as the observations in the stochastic inverse method (SIM) based on the maximum likelihood estimation procedure for the stochastic partial differential equation obtained by adding a noise term to the advection-dispersion equation. We have confined the estimation of dispersitivities to a flow length of 1 m (i.e, $x \in [0,1]$) except in Chapter 3, section 3.10, where we have estimated the dispersitivities up to 10 km using the SIM by simplifying the SSTM. This approach was proven to be computationally expensive and the approximation of the SSTM we have developed was based on the spatial average of the variance of the fluctuation term over the flow length. Further, the solution is based on a specific kernel. This development in Chapter 3 is inadequate to examine the scale dependence of the dispersivity. Therefore, we set out to develop a dimensionless model for any given arbitrary flow length, L , in this Chapter for any given velocity kernel provided that we have the eigen functions in the form given by equation (4.2.3). Then we examine the dispersivities in relation to the flow lengths to understand the multi-scale behaviour of the SSTM.

The starting point of the development of the multi-scale SSTM is the Langevin equation for the SSTM, which is interpreted locally. From equation (4.9.1), the Langevin equation can be written as,

$$dC_x(t) = -\alpha_x(C_x(t), \overline{V}(x,t), x)dt + \beta_x(C_x(t), \frac{\partial C_x}{\partial x}, \frac{\partial^2 C_x}{\partial x^2}, x)dw(t) \tag{6.1.1}$$

where the coefficients α_x and β_x are dependent on $x, C_x(t)$ and $\overline{V}(x,t)$; and $C_x(t), \frac{\partial C_x}{\partial x}, \frac{\partial^2 C_x}{\partial x^2}$ and x , respectively. $dw(t)$ are the standard Wiener increments with zero-mean and dt variance. As discussed in Chapter 4, equation (6.1.1) has to be interpreted carefully to understand it better. Equation (6.1.1) is a SDE and also an Ito diffusion with the coefficients depending on the functions of space variables. It gives us the time evolution of the concentration of solute at a given point x which is denoted by subscript x . Obviously, the computation of C_x also depends on how the spatial

Computational Modelling of Multi-Scale Non-Fickian Dispersion
in Porous Media - An Approach Based on Stochastic Calculus

178

derivatives of C_x are calculated. In that sense, equation (6.1.1) is a stochastic partial differential equation as the coefficients are functions of random quantities. But we avoid solving a SPDE by treating equation (6.1.1) as a SDE and interpreting it as an Ito integral which makes us to evaluate coefficients at the previous time point with respect to the current point of evaluation.

For simplicity, we will denote the coefficients as α_x and β_x. In Chapter 4, we have derived explicit function for α_x and β_x:

$$\alpha = C_x(t)F_{x,0} + \left(\frac{\partial C}{\partial x}\right)_x F_{x,1} + \left(\frac{\partial^2 C}{\partial x^2}\right)_x F_{x,2}. \tag{6.1.2}$$

Where

$$F_{x,0} = \frac{\partial \overline{V}(x,t)}{\partial x} + \frac{h_x}{2}\frac{\partial^2 \overline{V}(x,t)}{\partial x^2}, \tag{6.1.3}$$

$$F_{x,1} = \overline{V}(x,t) + h_x \frac{\partial \overline{V}(x,t)}{\partial x}, \tag{6.1.4}$$

and,

$$F_{x,3} = \frac{h_x}{2}\overline{V}(x,t); \tag{6.1.5}$$

$$\beta_x = \left(\beta_0^2 + \beta_1^2 + \beta_2^2\right)^{\frac{1}{2}}, \tag{6.1.6}$$

where,

$$\beta_0 = C_x(t)\sqrt{a_{00}}, \tag{6.1.7}$$

$$\beta_1 = \left(\frac{\partial C}{\partial x}\right)_x \sqrt{a_{11}}, \tag{6.1.8}$$

$$\beta_2 = \left(\frac{\partial^2 C}{\partial x^2}\right)_x \sqrt{a_{22}}, \tag{6.1.9}$$

and

$$a_{ii} = \sigma^2 \sum_{j=1}^{m} \lambda_j P_{ij}^2, \qquad (i,0,1,2), \tag{6.1.10}$$

In equation (6.1.10), σ^2 is the variance of the covariance kernel, λ_j are eigen functions, and for the domain of $x \in [0,1]$,

$$P_{0j}(x) = \left[g_{ij} - 2\sum_{k=2}^{p_j} g_{kj} r_{kj} \left(x - s_{kj}\right) e^{-r_{kj}\left(x-s_{kj}\right)^2} \right]$$
$$+ \left(\frac{h_x}{2}\right)\left[4\sum_{k=2}^{p_j} g_{kj} r_{kj}^2 \left(x - s_{kj}\right)^2 e^{-r_{kj}\left(x-s_{kj}\right)^2} - 2\sum_{k=2}^{p_j} g_{kj} r_{kj} e^{-r_{kj}\left(x-s_{kj}\right)^2} \right], \quad (6.1.11)$$

$$P_{1j}(x) = g_{0j} + g_{1j}x + \sum_{k=2}^{p_j} g_{kj} e^{-r_{kj}\left(x-s_{kj}\right)^2}$$
$$+ \left(\frac{h_x}{2}\right)\left[2\left(g_{ij} - 2\sum_{k=2}^{p_j} g_{kj} r_{kj} \left(x - s_{kj}\right) e^{-r_{kj}\left(x-s_{kj}\right)^2} \right) \right], \quad (6.1.12)$$

and

$$P_{2j}(x) = \left(\frac{h_x}{2}\right)\left[g_{0j} + g_{1j}x + \sum_{k=2}^{p_j} g_{kj} e^{-r_{kj}\left(x-s_{kj}\right)^2} \right]. \quad (6.1.13)$$

Equation (6.1.1) to (6.1.13) constitute the Langevin form of the SSTM. It should be noted that the functions P_{ij} are only valid for $x \in [0,1]$. If we normalize the spatial variable x to remain with in $[0,1]$, then we can use the results in Chapter 4 to obtain P_{ij}. We develop the dimensionless Langevin form of the SSTM in section 6.2.

One should note that the Langevin equation for any system reflect the role of external noise to the system under consideration (van Kampen, 1992). Even though we have derived equation (6.1.1) starting from the mass conservation of solute particles, the fluctuations associate with hydrodynamics dispersion are a result of dissipation of energy of particles due to momentum changes associated near to the surfaces of porous medium. For α physical ensemble of solute particles, porous medium through which it flows act as an external source of noise. From this point of review, the Langevin type equation for solute concentration is justified. As a SDE, equation (6.1.1) is a Wiener process with stochastic, at best nonlinear, time-dependent coefficients, and it is also an Ito diffusion which should be interpreted locally, i.e., for a given x and t, equation (6.1.1) is valid only for short time intervals beyond t. This naturally leads us to evaluate the associated spatial derivatives at the previous time, which is valid according to Ito's interpretation of stochastic integral. In terms of discretized times, $t_0, t_1, \ldots, t_i, t_{i+1}, \ldots,$ equation (6.1.1) can be written as,

$$dC_x(t) = C_x(t+1) - C_x(t) = \alpha_x\left(C_x(t_i), \bar{V}(x,t_i), \left(\frac{\partial \bar{V}}{\partial x}\right)_{t_i}, \left(\frac{\partial^2 \bar{V}}{\partial x^2}\right)_{t_i} \right)(t_{i+1} - t_i)$$
$$+ (\beta_x)\left(C_x(t_i), \bar{V}(x,t_i), \left(\frac{\partial \bar{V}}{\partial x}\right)_{t_i}, \left(\frac{\partial^2 \bar{V}}{\partial x^2}\right)_{t_i} \right) d\omega(t_i) \quad (6.1.14)$$

where the drift coefficient, α_x, and the diffusion coefficient, β_x, are evaluated at time $= t_i$. This restrictive nature of equation (6.1.14) in evaluating the coefficient has to be taken in to account in developing numerical algorithms to solve it.

6.2 Partially Dimensionless SSTM with Flow Length L

We start the derivation of partially dimensionless SSTM by defining the dimensionless distance, Z, as:

$$Z = \frac{x}{L} \tag{6.2.1}$$

where L is the total flow length.

When $x \in [0, L]$, $Z \in [0, 1]$.

If C_0 is a constant concentration defined such a way that $C_0 = $ maximum of $C_x(t)$ for all x and t, then $C_0 \geq C_x(t)$ for any t and x. We can define dimensional concentration $\Gamma(t)$ as,

$$\Gamma(t) = \frac{C_x}{C_0} \quad . \tag{6.2.2}$$

From equation (6.2.1),

$$\frac{\partial Z}{\partial x} = \frac{1}{L}, \tag{6.2.3a}$$

$$\frac{\partial C_x}{\partial x} = \frac{\partial (C_0 \Gamma)}{\partial Z} \cdot \frac{\partial Z}{\partial x} = \frac{C_0}{L} \frac{\partial \Gamma}{\partial Z}, \tag{6.2.3b}$$

$$\frac{\partial^2 C_x}{\partial x^2} = \frac{\partial}{\partial x}\left(\frac{\partial C_x}{\partial x}\right) = \frac{\partial}{\partial x}\left(\frac{C_0}{L}\frac{\partial \Gamma}{\partial Z}\right) = \frac{\partial}{\partial Z}\left(\frac{C_0}{L}\frac{\partial \Gamma}{\partial Z}\right) \cdot \frac{\partial Z}{\partial x} = \frac{C_0}{L^2}\frac{\partial^2 \Gamma}{\partial Z^2}. \tag{6.2.3c}$$

As the domain of x is the generalized SSTM is from 0 to 1, we can replace x with Z in the dimensionless generalized SSTM. For example, $F_{x,0}$ becomes $F_{Z,0}$.

$$\begin{aligned}
F_{Z,0} &= \frac{\partial \overline{V}(Z,t)}{\partial x} + \frac{h_z}{2}\frac{\partial^2 \overline{V}(Z,t)}{\partial x^2} = \frac{\partial \overline{V}(Z,t)}{\partial Z} \cdot \frac{\partial Z}{\partial x} + \frac{h_z}{2}\frac{\partial}{\partial x}\left(\frac{\partial \overline{V}}{\partial Z} \cdot \frac{\partial Z}{\partial x}\right) \\
&= \frac{1}{L}\frac{\partial \overline{V}}{\partial Z} + \frac{h_z}{2L}\frac{\partial}{\partial Z}\left(\frac{\partial \overline{V}}{\partial Z}\right)\left(\frac{\partial Z}{\partial x}\right) = \frac{1}{L}\frac{\partial \overline{V}}{\partial Z} + \frac{h_z}{2L^2}\frac{\partial^2 \overline{V}}{\partial Z^2}.
\end{aligned} \tag{6.2.4}$$

Similarly,

$$F_{Z,1} = \overline{V}(Z,t) + \frac{h_z}{L}\frac{\partial \overline{V}}{\partial Z}; \text{ and} \tag{6.2.5}$$

$$F_{Z,2} = \frac{h_z}{2}\overline{V}(Z,t). \tag{6.2.6}$$

$P_{0j}(Z), P_{1j}(Z)$ and $P_{2j}(Z)$ are obtained by simply replacing x in $P_{0j}(x), P_{1j}(x)$ and $P_{2j}(x)$ expressions by Z, because these expressions are derived for $[0,1]$ domain.

Similarly,

$$\beta_0(Z) = C_0 \Gamma(t) \sqrt{a_{00}(Z)} \tag{6.2.7}$$

$$\beta_1(Z) = \frac{C_0}{L} \frac{\partial \Gamma}{\partial Z} \sqrt{a_{11}(Z)}, \text{ and} \tag{6.2.8}$$

$$\beta_2(Z) = \frac{C_0}{L^2} \frac{\partial^2 \Gamma}{\partial Z^2} \sqrt{a_{22}(Z)} \tag{6.2.9}$$

Now we can write equation (6.1.1) in the following manner:

$$d(C_0 \Gamma) = -\alpha_Z(Z) dt + \beta_Z(Z) d\omega(t), \tag{6.2.10}$$

$$d\Gamma = \frac{-\alpha Z(Z)}{C_0} dt + \frac{\beta_z(Z)}{C_0} d\omega(t). \tag{6.2.11}$$

where

$$\frac{\alpha_Z(Z)}{C_0} = \Gamma F_{Z,0} + \frac{1}{L} \frac{\partial \Gamma}{\partial Z} F_{Z,1} + \frac{1}{L^2} \frac{\partial^2 \Gamma}{\partial Z^2} F_{Z,2}, \tag{6.2.12}$$

$$\frac{\beta_Z(Z)}{C_0} = \left\{ \left(\Gamma^2 a_{00}(Z) \right) + \frac{1}{L^2} \left(\frac{\partial \Gamma}{\partial Z} \right)^2 a_{11}(Z) + \frac{1}{L^4} \left(\frac{\partial^2 \Gamma}{\partial Z^2} \right)^2 a_{22}(Z) \right\}^{\frac{1}{2}} \tag{6.2.13}$$

Therefore, the Langevin form of the generalized SSTM is given by

$$d\Gamma = -\alpha_Z dt + \beta_Z d\omega(t), 0 \le Z \le 1. \tag{6.2.14}$$

where $\bar{\alpha}_Z = \frac{\alpha_Z(Z)}{C_0}$ and $\bar{\beta}_Z = \frac{\beta_Z(Z)}{C_0}$.

Using equation (6.2.14) we can compute the time course of the dimensionless concentration for any given L.

The dimensionless/concentration, Γ, varies from 0 to 1. $C_Z(t)$ is proportioned to the number of solute moles within a unit volume of porous/water matrix, and C_0 is proportional to the maximum possible number of solute moles within the same matrix. Therefore, $\Gamma = C_Z(t)/C_0$ can be interpreted as the likelihood (probability) of finding solute moles within the matrix.

It should be noted that time, t, is not a dimensionless quantity and therefore, equation (6.2.14) is partially dimensionless equation. We will explore the dispersivity using equation (6.2.14) first before discussing a completely dimensionless equation.

6.3 Computational Exploration of the Langevin form of SSTM

Equation (6.2.14) is not only an expression of how the solute disperses within a porous media but also an expression of nature of dispersion. Being a SDE, the drift coefficient $\left(\bar{\alpha}_Z\right)$ portrays the dispersion due to the convective forces and the diffusive coefficient $\left(\bar{\beta}_Z\right)$ shows the dynamical behaviour of hydrodynamic dispersion. As Z has the range from 0 to 1 in equation (6.2.14), we can compute α_Z and β_Z values for a specific Z value and examine how they change over time. (We use $C_0 = 1.0$ for computations, and therefore, $\bar{\alpha}_Z = \alpha_Z$ and $\bar{\beta}_Z = \beta_Z$.) We have developed a finite difference algorithm to compute α_Z and β_Z adhering to the Ito integration as we have done before. Figure 6.1a and 6.1b show the time courses of $-\alpha_Z$ and β_Z at $Z = 0.5$, respectively, for different σ^2 values when $L = 1m$ (All times are given in days and $b = 0.1$. At low σ^2 values, $-\alpha_Z$ behaves almost as a smooth deterministic function but at high σ^2 values it shows irregular behaviours. In these calculations, we have kept the mean velocity $\bar{V}$ at a constant value (0.5), therefore only fluctuating component affecting α_Z function is the solute concentration and its spatial derivatives. Further, Figure 6.1a and 6.1b only show a single realization for each σ^2 values. When we explore multiple realizations (not shown here), we see that randomness of α_Z and β_Z increases with higher σ^2. One distinct feature of Figure 6.1b for β_Z is that β_Z is almost negligible for very small values of σ^2 but increases quite sharply for higher σ^2 values. α_Z does not behave in this manner. However, we can not ignore the effect of σ^2 at low values in computing $\Gamma(Z)$, which has a follow-on affect on subsequent calculation. In other words, the affects of porous media, which σ^2 and the covariance kernel signify, can not be ignored as they affect the flow velocities significantly in making them stochastic. Figure 6.2a and 6.2b show $-\alpha_Z$ and β_Z realization at $Z = 0.5$ when $L = 5m$. The behaviours of $-\alpha_Z$ and β_Z realizations are similar to those shown in Figures 6.1a and 6.1b. Figure 6.3a and Figure 6.3b show the similar trends for $L = 10m$. It should be noted that as L is increased, the time duration for the numerical solution of equation (6.2.14) should be increased. For example, when $L = 10m$, the model was run for 25 days to obtain Figures 6.3a and 6.3b. However, the order of magnitude for α_Z and β_Z has not changed as we change L in an order of magnitude.
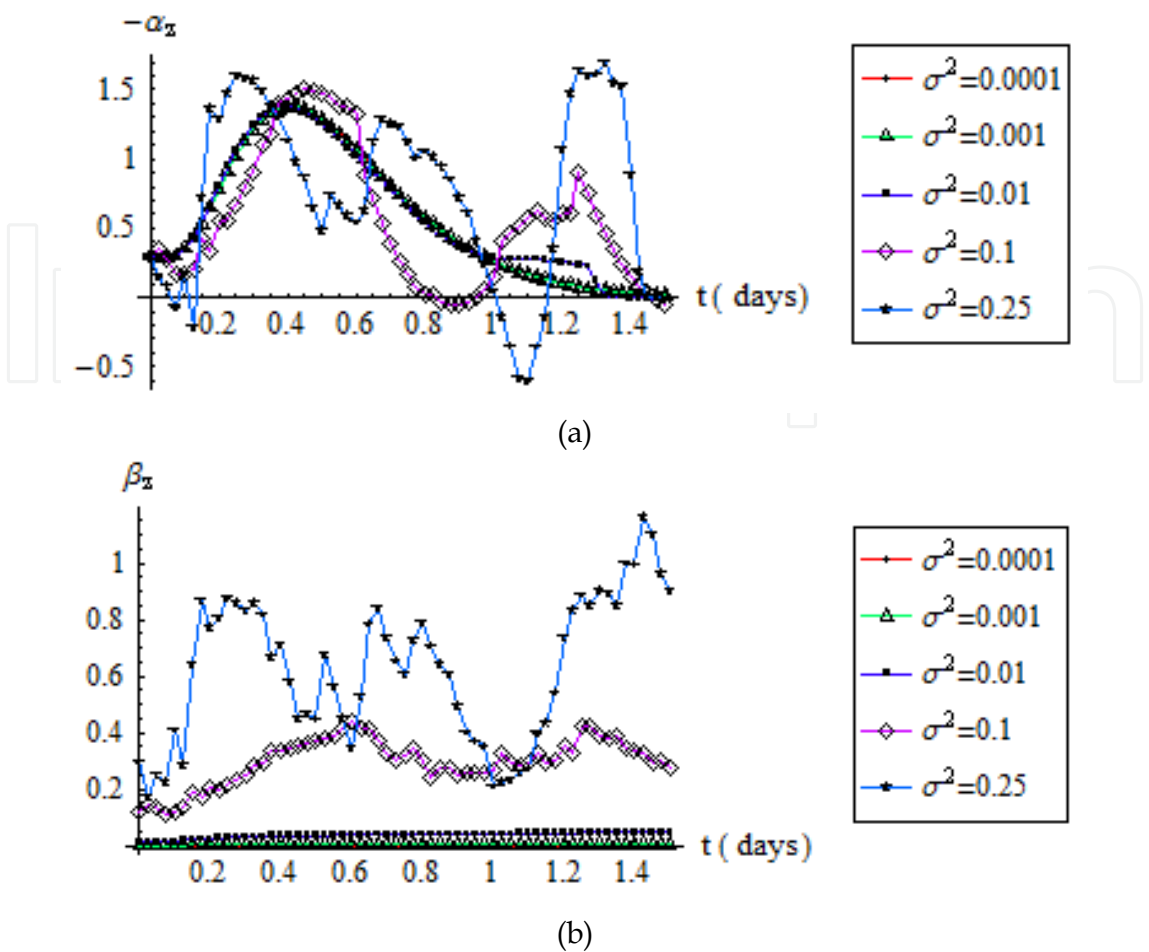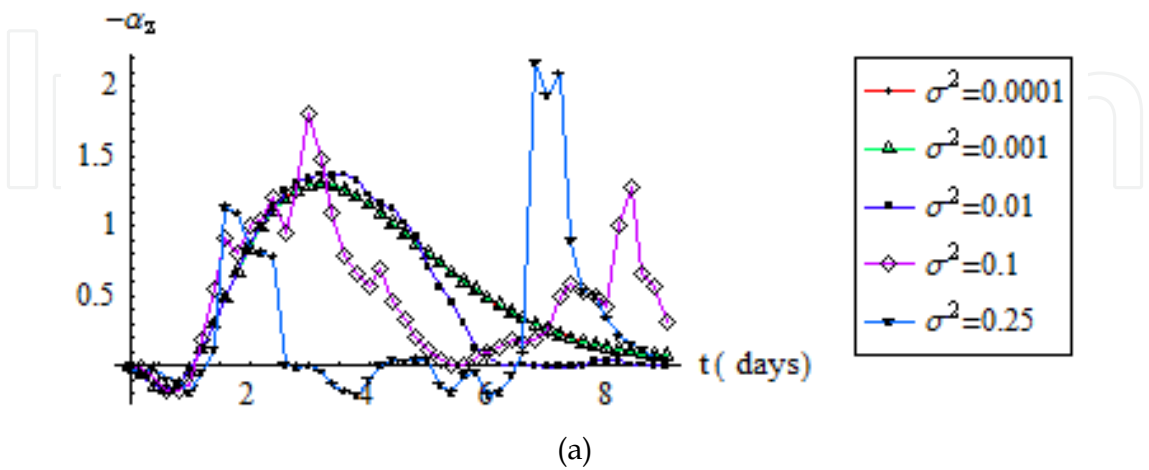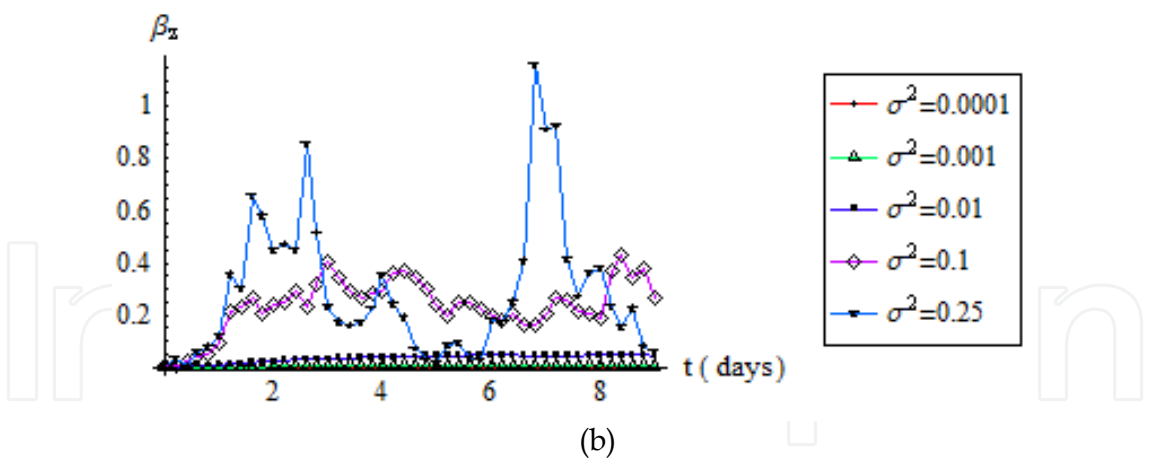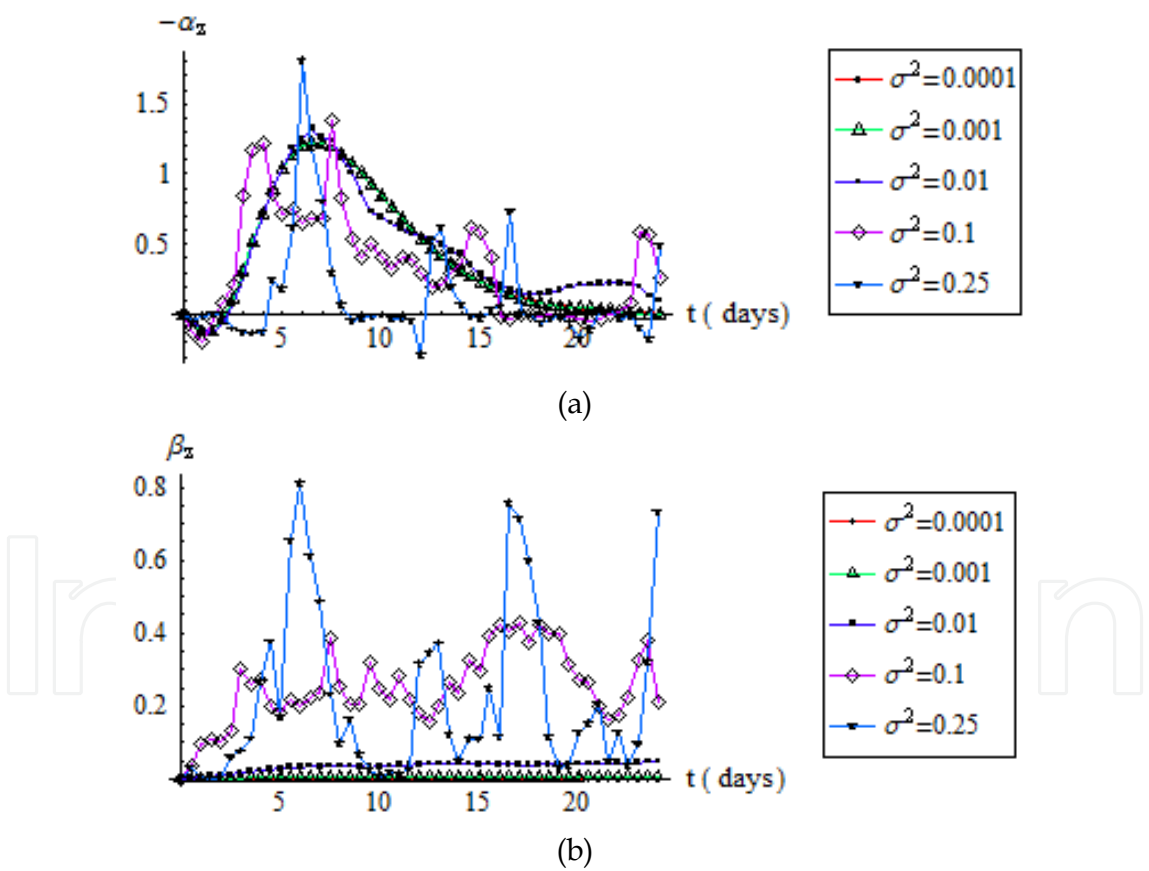
(a)

(b)

Figure 6.1. (a) Realizations of $-\alpha_Z$ at $Z = 0.5$ when $L = 1\,m$, $b = 0.1$ and $\bar{V} = 0.5\,m/day$ for different σ^2 values; (b) Realizations of β_Z at $Z = 0.5$ when $L = 1\,m$, $b = 0.1$ and $\bar{V} = 0.5\,m/day$ for different σ^2 values.

(a)

184

Computational Modelling of Multi-Scale Non-Fickian Dispersion
in Porous Media - An Approach Based on Stochastic Calculus

(b)

Figure 6.2. (a) Realizations of $-\alpha_Z$ at $Z = 0.5$ when $L = 5m$, $b = 0.1$ and $\bar{V} = 0.5\,m\,/\,day$ for different σ^2 values; (b) Realizations of β_Z at $Z = 0.5$ when $L = 5m$, $b = 0.1$ and $\bar{V} = 0.5\,m\,/\,day$ for different σ^2 values.

(a)

(b)

Figure 6.3. (a) Realizations of $-\alpha_Z$ at $Z = 0.5$ when $L = 10$ m, $b = 0.1$ and $\bar{V} = 0.5$ m/day for different σ^2 values; (b) Realizations of β_Z at $Z = 0.5$ when $L = 10$ m, $b = 0.1$ and $\bar{V} = 0.5$ m/day for different σ^2 values.
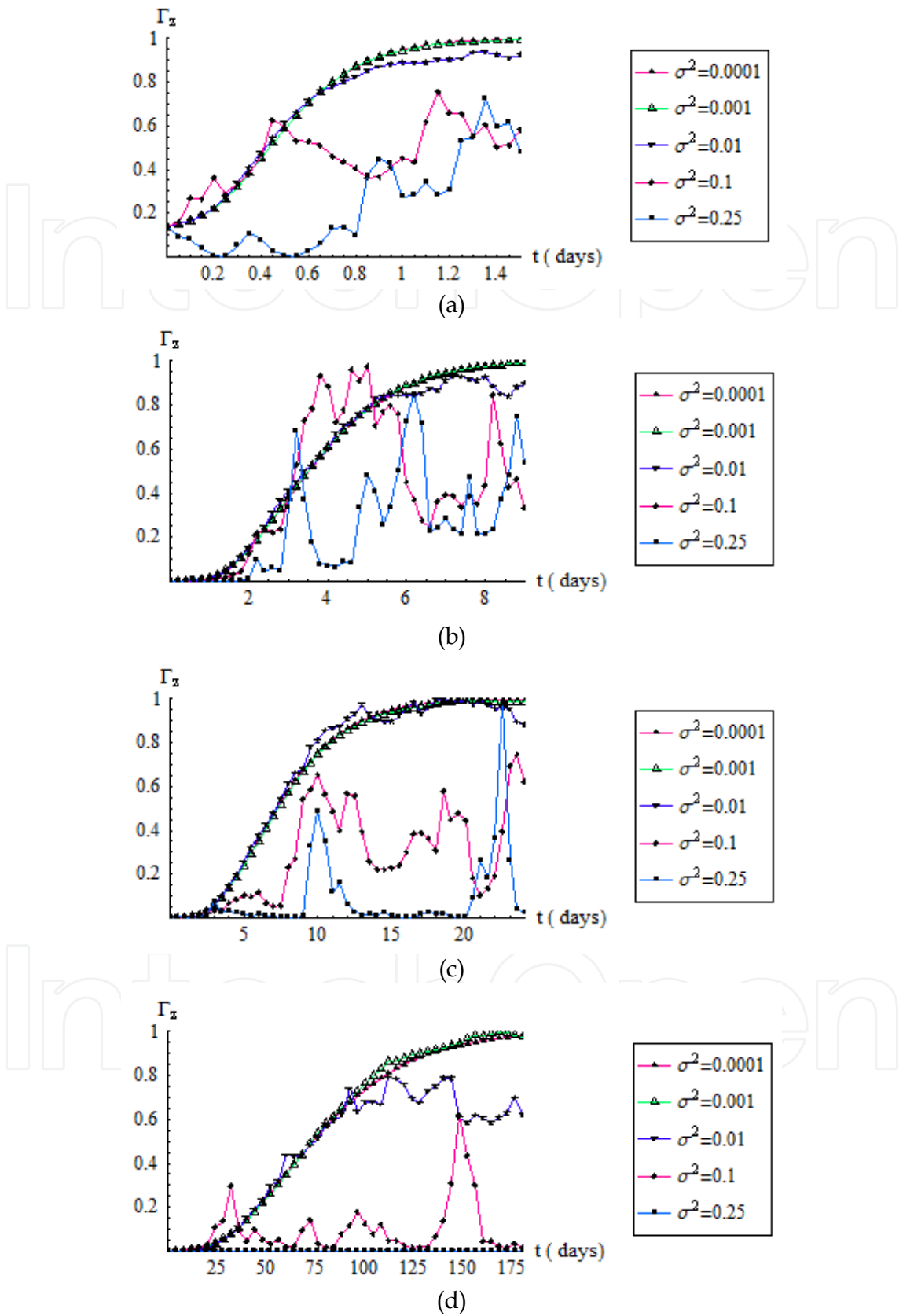
Figure 6.4. Realizations of Γ_Z at $Z = 0.5$ when $b = 0.1$, $\bar{V} = 0.5$ for (a) $L = 1$, (b) $L = 5$, (c) $L = 10$ and (d) $L = 100$

186

Computational Modelling of Multi-Scale Non-Fickian Dispersion
in Porous Media - An Approach Based on Stochastic Calculus

Figure 6.4a, 6.4b, 6.4c, and 6.4d show the realization of $\Gamma(Z)$ at $Z = 0.5$ when $L = 1, 5, 10,$ and 100, respectively, for different values of σ^2. (For all the calculations, we have used $b = 0.1$). When $L = 100$ m, we computed $\Gamma(Z)$ values for 175 days and the affects of σ^2 on $\Gamma(Z)$ is quite dramatic, and this shows that equation (6.2.14) can display very complex behaviour patterns albeit its simplicity. It should be noted however that σ^2 plays major role in delimiting the nature of realizations; σ^2 values high than 0.25 in these situations produces highly irregular concentration realizations which could occur in highly heterogeneous porous formations such as fractured formations.

6.4 Dispersivities Based on the Langevin Form of SSTM for $L \leq 10$ m

One of the advantages of the partially dimensionless Langevin equation for the SSTM (equation 6.2.14) is that we can use it to compute the solute concentration profiles when the travel length (L) is large. Equation (6.2.14) allows us to compute the dispersitivities using the stochastic inverse method (SIM) by estimating dispersivity for each realization of $\Gamma(Z)$. For the SIM, we need to modify the deterministic-advection and dispersion equation into a partially dimensionless one. We start with the deterministic advection-dispersion equation with additive Gaussian noise,

$$\frac{\partial C}{\partial t} = D_L \frac{\partial^2 C}{\partial x^2} - V_x \frac{\partial C}{\partial x} + \xi(x,t), \tag{6.4.1}$$

where D_L is the dispersion coefficient (dispersivity $\times V_x$).

The partially dimensionless form of equation (6.4.1) is,

$$\frac{\partial \Gamma}{\partial t} = \frac{D_L}{L^2} \frac{\partial^2 \Gamma}{\partial Z^2} - \frac{V_x}{L} \frac{\partial \Gamma}{\partial Z} + \xi(Z,t), \tag{6.4.2}$$

where $\dfrac{D_L}{L^2}$ is now estimated using SIM when V_x is known. Then the dispersivity value is (estimated $\dfrac{D_L}{L^2}$) $\times L^2 / V_x$.

Figure 6.5 show the scatter plots of dispersivity values estimated using the SIM for $L = 1, 5,$ and 10 m. Each plot in Figure 6.5 gives 30 estimates of the dispersivity for a given value σ^2. $\Gamma(Z)$ realizations were computed at $Z = 0.5$ and $b = 0.1$ for all plots. Table 6.1 summarizes the results giving the mean of each plot. We will compare these results with available data for dispersivities later in this chapter.
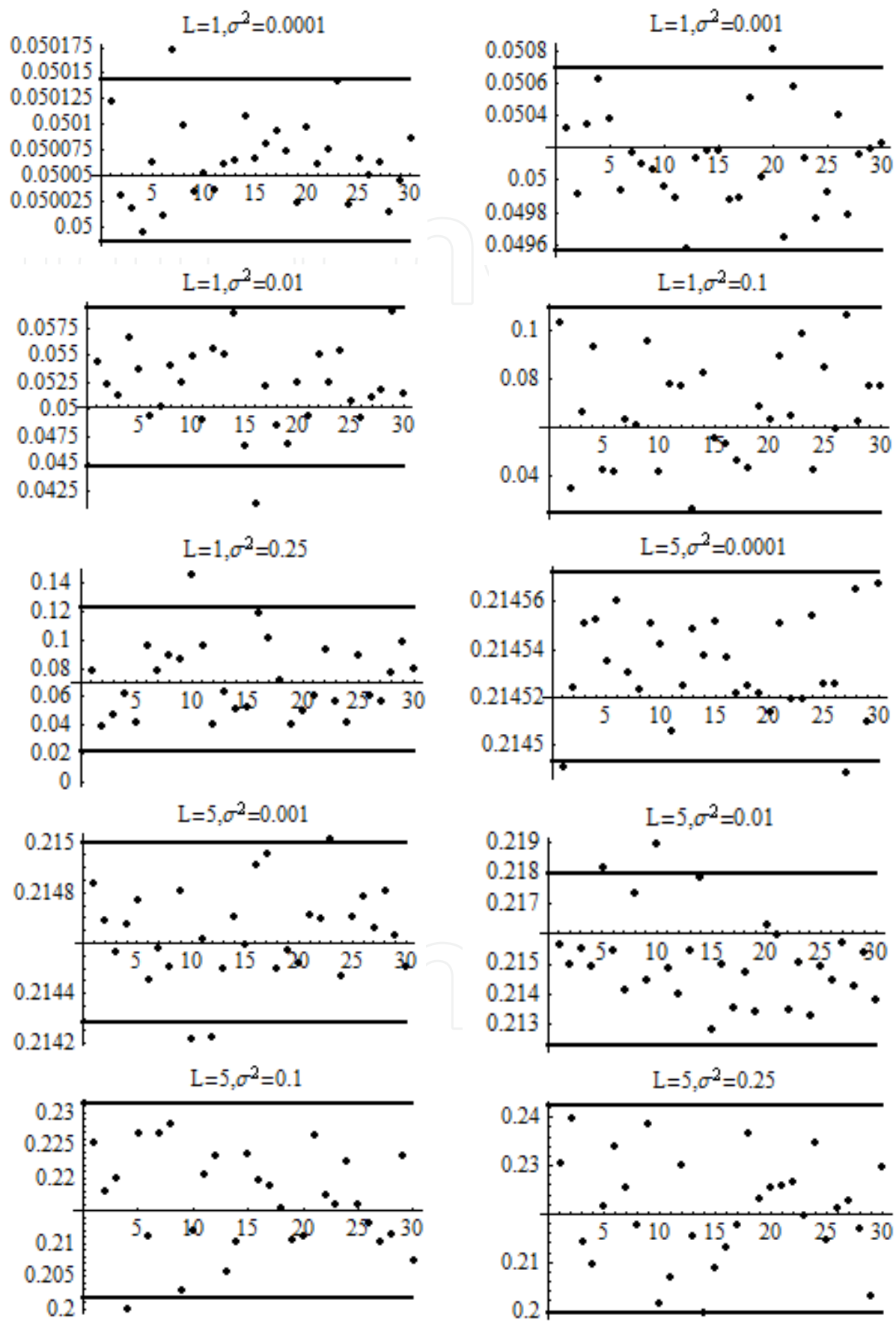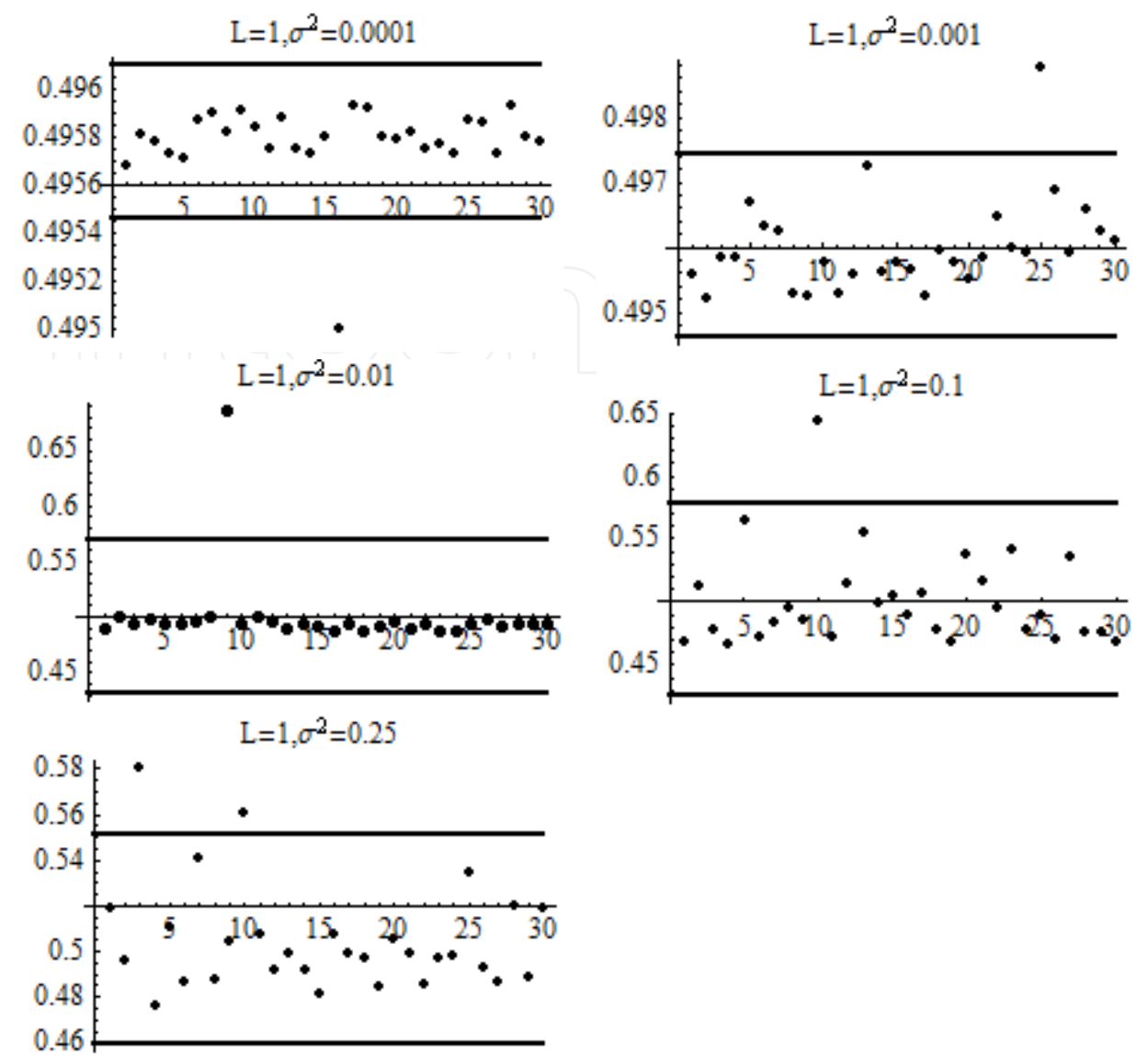
Figure 6.5. Dispersivities estimated from SSTM for $L = 1, 5$, and 10.

σ^2	Dispersivity		
	L=1	L=5	L=10
0.0001	0.050064	0.050112	0.0495545
0.001	0.0501232	0.05082	0.0511587
0.01	0.0520638	0.0604215	0.0778382
0.1	0.0669766	0.0832735	0.11899
0.25	0.0723413	0.111142	0.253195
0.4	0.0783754	0.142422	0.354335
0.6	0.0843219	0.170975	0.427603
0.8	0.0962623	0.225344	0.549473
1	0.110849	0.256348	0.609508

Table 6.1. Mean dispersivities for the data in Figure 6.5.

As mentioned previously, the partially dimensionless equation (6.2.14) still requires us to compute for a large number of days when L is large. While the computational times are still manageable, we would like to develop a completely dimensionless Langevin equation for the SSTM. This could be especially useful and insightful when the mean velocity $\bar{V}$ could be considered as a constant.

6.5 Dimensionless Time

We introduce dimensionless time, θ, as,

$$\theta = \bar{V}(Z,t).\frac{t}{L}, \tag{6.5.1}$$

where, $\bar{V}(Z,t)$ is mean velocity when $0 \leq Z \leq 1$, (m/day); L is travel length, m; and t is time in days.

Therefore, if $\bar{V} = 0.5$, $L = 100$ and $0 \leq t \leq 200$, then, $0 \leq \theta \leq 1.0$. This allows us to compute $\Gamma(Z)$ realization for larger times.

Equation (6.2.14) can be written as,

$$\Gamma(Z) = -\alpha_Z dt + \beta_z d\omega(t).$$

We can now change $dt = \frac{L}{\bar{V}}d\theta$, and the variance of $d\omega(t) = \Delta t = \frac{L}{\bar{V}}\Delta\theta$.

Therefore,

$$\Gamma(Z) = \frac{-\alpha_Z L}{\bar{V}}d\theta + \beta_z d\omega(t), \tag{6.5.2}$$

where $dw(\theta) \sim \mathrm{N}\left(0, \frac{L}{\bar{V}}d\theta\right)$.

The completely dimentionless Langevin form of the SSTM is therefore,

$$\Gamma(Z) = \alpha_{Z,\theta}d\theta + \beta_z d\omega(\theta), \tag{6.5.3}$$

where $d\omega(\theta)$ are the Wiener increment with zero-mean and $\frac{L}{\bar{V}}d\theta$ variance, and

$$\alpha_{Z,\theta} = \frac{-\alpha_Z L}{\bar{V}}. \tag{6.5.4}$$

To use equation (6.5.3), we need to choose $\Delta\theta$ and the range of θ appropriately. Ideally $\frac{L}{\bar{V}}d\theta < 0.0001$ for the Ito integration to be accurate; therefore, we should have for maximum $\Delta\theta$ as $\frac{0.0001\bar{V}}{L}$. Suppose $\bar{V} = 0.5, L = 1000$, then $\Delta\theta < \frac{10^{-4} \times 0.5}{1000}$, i.e, $\Delta\theta < 5 \times 10^{-8}$.

Computational Modelling of Multi-Scale Non-Fickian Dispersion
in Porous Media - An Approach Based on Stochastic Calculus

190

As we can see we may not gain much computational advantage with a completely dimensionless Langevin form of the SSTM.

6.6 Estimation of Field Scale Dispersivities

We have estimated the longitudinal dispersivities using SSTM for two different boundary conditions:

(A) $\Gamma_Z = 1$ at $Z = 0$ and for $t \geq 0;$ and

(B) $\Gamma_Z = 1$ at $Z = 0$ and for $0 \leq t \leq t_R$, ; and $\Gamma_Z = 0$ at $Z=0$ for $t > t_R$.

t_R is taken to be 1/3 of the total time (T) of the computational experiment. Table 6.1 and 6.2 show the dispersivity values for the boundary conditions A and B, respectively, when $L \leq 10$ m based on 100 realisations for each of the boundary condition.

σ^2	Dispersivity		
	L=1	L=5	L=10
0.0001	0.050013	0.050013	0.049828
0.001	0.050035	0.050223	0.050226
0.01	0.050646	0.055152	0.06112
0.1	0.055176	0.079403	0.136904
0.25	0.068846	0.108899	0.257902
0.4	0.083342	0.16346	0.333472
0.6	0.093185	0.191919	0.334818
0.8	0.109335	0.251033	0.54346
1	0.129395	0.331389	0.613823

Table 6.2. Longitudinal dispersivities (mean) for the boundary condition A.

The values in Table 6.1 and 6.2 are similar for the similar values of σ^2 and L showing that (1) the SSTM procedure is robust in evaluating the dispersivities, and (2) the computed mean dispersivities do not depend on the boundary conditions, A and B. In these calculations, we have $\bar{V}_Z = 0.5$ m/day.

We have also computed the dispersivities for larger scales up to 10,000 m, and Table 6.3 gives the mean values for the range of L from 1 m to 10^4 m under the boundary condition A, and Table 6.4 gives the mean values for the range of L from 1 m to 10^8 m for the boundary condition B. All mean values are calculated based on different sets of 100 realisations for each boundary condition. Except for the smallest σ^2 values (0.0001 and 0.001), the dispersivities have similar mean values for both boundary conditions, A and B. Therefore, it is quite reasonable to compute the dispersivities only for the boundary condition A for larger values of L. We can also hypothesise that the dispersivities are independent of the boundary conditions used to solve the SSTM. We have tested the SSTM for different values of $t_R > (1/3)$ T when $L>10$ m. Figure 6.6 depicts the dispersivity plotted against σ^2 and L in Log10 scale, and Log10 (Dispersivity) is a linear function of Log10(L)

and Log10(σ^2) for the most parts of the Log10 (Dispersivity) surface. Figure 6.7 shows the linear relationship of Log10 (Dispersivity) vs Log10 (L) for different values of σ^2, and Figure 6.8 shows the same for Log10 (Dispersivity) vs Log10(σ^2) for different values of L. The gradient of the graphs are the same except for lower values of σ^2 (0.0001) and lower values of L (1 and 5). Therefore, we develop the following statistical nonlinear regression models for these significant relationships:

$$D_s = C_1\left(\sigma^2\right)^{m1}, \text{ and} \tag{6.6.1}$$

$$D_s = C_2\left(L\right)^{m2}, \tag{6.6.2}$$

where D_s is the dispersivity, and C_1 and C_2 are given in Tables 6.5 and 6.6 , respectively, along with *m1* and *m2* values. R-square values for equations (6.6.1) and (6.6.2) are 0.96 and 0.94, respectively.

σ^2	Dispersivity					
	L=1	L=5	L=10	L=50	L=100	L=500
0.0001	0.0498	0.0500	0.0497	0.0498	0.0507	0.0686
0.001	0.0498	0.0499	0.0495	0.0477	0.0639	0.4982
0.01	0.0492	0.0510	0.0511	0.1642	0.5073	4.0672
0.1	0.0449	0.0592	0.1372	0.9309	2.9601	28.6151
0.25	0.0451	0.1123	0.2391	2.5441	6.1225	40.5301
0.4	0.0573	0.1340	0.3413	3.4365	8.1834	48.7567
0.6	0.0784	0.1824	0.4619	4.9440	10.9837	64.7589
0.8	0.0958	0.1987	0.7057	6.6800	14.9122	82.4423
1	0.1247	0.2159	0.8102	8.9878	19.9003	112.5246
	L=1000	L=2000	L=4000	L=6000	L=8000	L=10000
0.0001	0.2697	0.7964	2.0630	4.1138	5.9939	8.1065
0.001	2.5154	7.2616	20.5460	32.6517	45.9978	69.0446
0.01	12.6500	30.0361	81.0270	155.2103	231.3154	324.3036
0.1	70.0564	156.8923	333.6665	523.4295	708.0212	903.6889
0.25	87.8303	185.7131	381.1019	569.9892	766.8287	978.5914
0.4	101.1441	203.0552	425.5467	625.6709	866.0189	1061.9651
0.6	131.0882	259.4990	528.0956	828.7496	1079.0040	1355.8468
0.8	173.1833	344.9935	691.7747	1070.9582	1399.5126	1771.3449
1	227.3204	453.3977	925.0844	1396.8663	1864.1378	2337.5588

Table 6.3. Longitudinal dispersivities (mean) for the range of L from 1 m to 10^4 m under the boundary condition A

σ^2	Dispersivity						
	L=1	L=5	L=10	L=50	L=100	L=500	L=1000
0.0001	0.0498	0.0500	0.0497	0.0498	0.0507	0.0686	0.1426
0.001	0.0498	0.0499	0.0495	0.0477	0.0639	0.4982	1.4690
0.01	0.0492	0.0510	0.0511	0.1642	0.5073	4.0672	12.0999
0.1	0.0449	0.0592	0.1372	0.9309	2.9601	28.6151	69.2489
0.25	0.0451	0.1123	0.2391	2.5441	6.1225	40.5301	87.0760
0.4	0.0573	0.1340	0.3413	3.4365	8.1834	48.7567	100.6075
0.6	0.0784	0.1824	0.4619	4.9440	10.9837	64.7589	132.1320
0.8	0.0958	0.1987	0.7057	6.6800	14.9122	82.4423	173.1823
1	0.1247	0.2159	0.8102	8.9878	19.9003	112.5246	221.6737

Table 6.4. Longitudinal dispersivities (mean) for the range of L from 1 m to 10^8 m under the boundary condition B
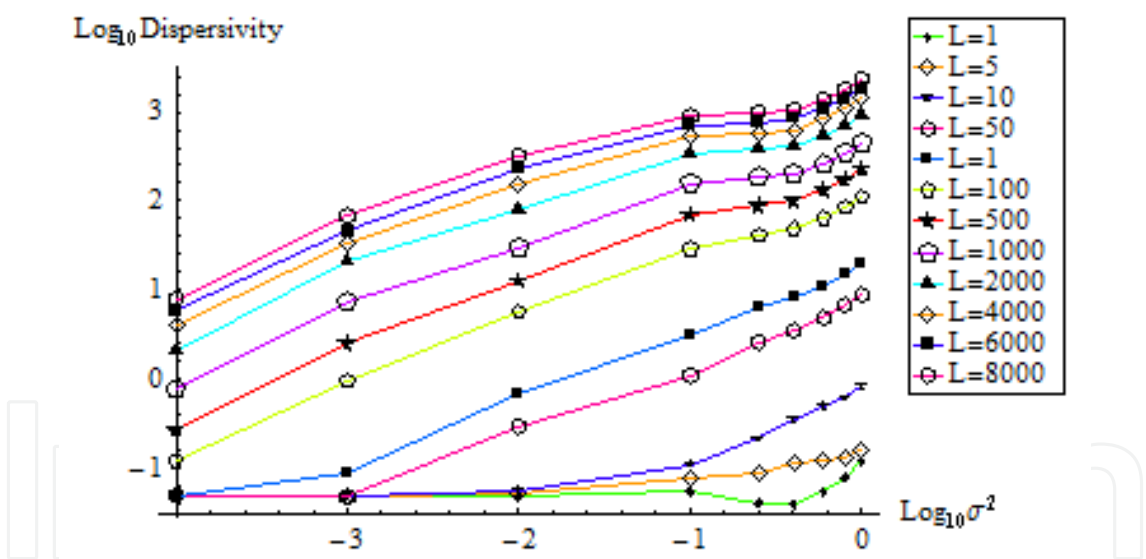
Figure 6.6. The linear relationship of Log10 (Dispersivity) vs Log10 (σ^2) for different values of L.
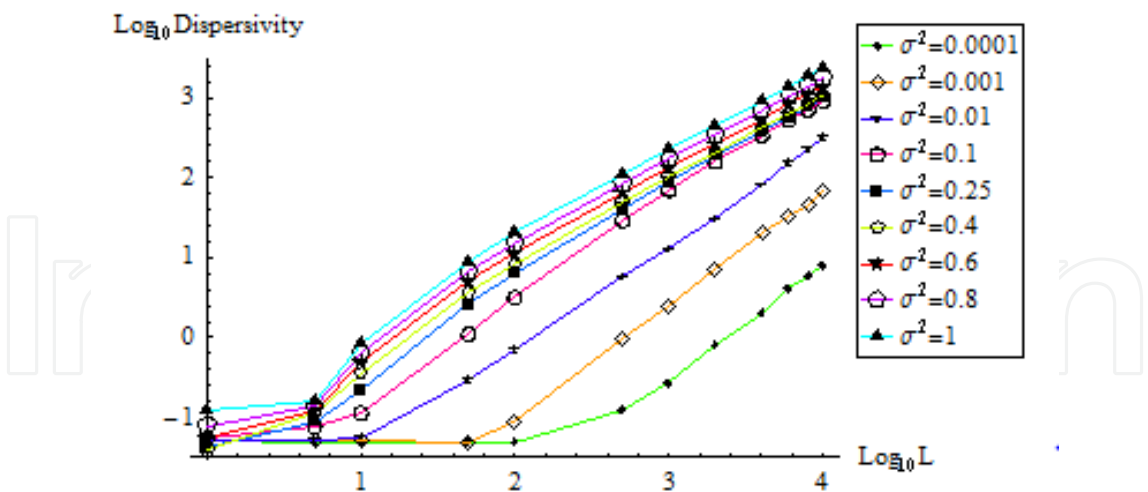
Figure 6.7. The linear relationship of Log10 (Dispersivity) vs Log10 (L) for different values of σ^2.
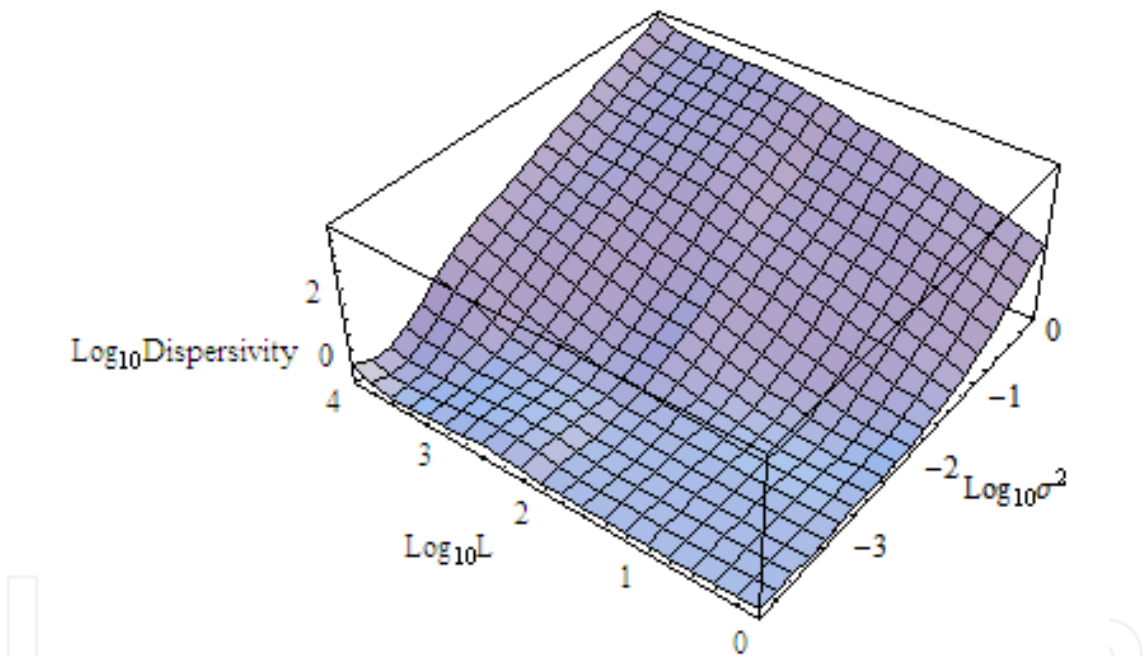
Figure 6.8. The plot of Log10 (Dispersivity) vs Log10 (σ^2) and Log10 (L)

L (m)	1	5	10	50	100	500
m1	0.039	0.125	0.311	0.605	0.677	0.704
C_1	0.063	0.124	0.468	6.275	16.23	109.6
L (m)	1000	2000	4000	6000	8000	10000
m1	0.690	0.642	0.605	0.578	0.567	0.552
C_1	229.5	451.3	912.4	1368.7	1823.1	2281.4

Table 6.5. *m1* and C_1 values for different L for equation (6.6.1).

σ^2	0.0001	0.001	0.01	0.1	0.25	0.4	0.6	0.8	1.0
m2	0.589	0.897	1.067	1.150	1.148	1.148	1.148	1.148	1.144
C_2	0.0122	0.0078	0.0103	0.0168	0.0242	0.0311	0.0409	0.0535	0.0725

Table 6.6. *m2* and C_2 values for different σ^2 for equation (6.6.2).
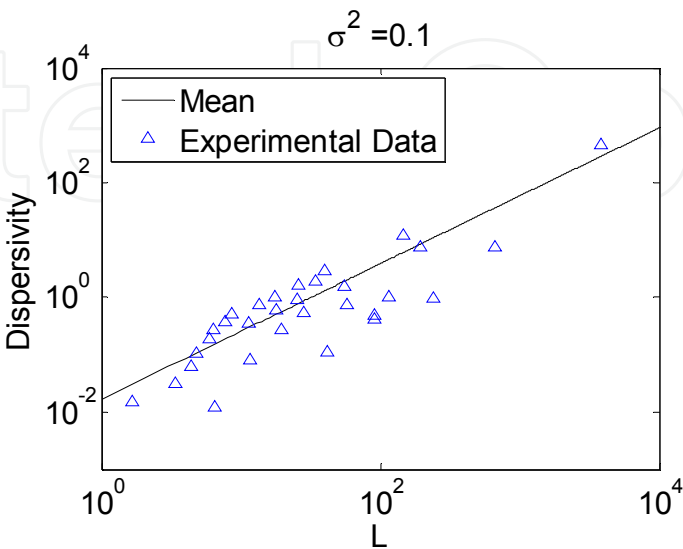
Figure 6.9. Mean dispersivity from the SSTM and experimental dispersivity vs flow length (log10 scale).

We can estimate the approximate dispersivity values either from Figures 6.7 and 6.8, or from equations (6.6.1) and (6.6.2). It is quite logical to ask the question whether we can characterise the large scale aquifer dispersivities using a single value of σ^2? To answer this question, we resort to the published dispersivity values for aquifers. We use the dispersivity data first published by Gelhar et al. (1992) and reported to Batu (2006). We extracted the tracer tests data related to porous aquifers in 59 different locations characterised by different geologic materials. The longest flow length was less than 10000 m. We then plotted the experimental data and overlaid the plot with the dispersivity vs L curves from the SSTM for each σ^2 value. Figure 6.9 shows the plots, and σ^2 =0.1 best fit to the experimental data. In other words, by using one value of σ^2, we can obtain the dispersivity for any length of the flow by using the SSTM. We can also assume that each experimental data point represents the mean dispersivity for any length of the flow by using the SSTM. We can also assume that each experimental data point represents the mean dispersivity at a particular flow length. If that is the case, Figure 6.9 can be interpreted as follows: by using the SSTM, we can obtain sufficiently large number of realisations for particular values of σ^2 and the mean flow velocity, and the mean values of the dispersivities estimated for those concentration realisations do represent the experimental dispersivities. σ^2 can be hypothesised to indicate the type of media (e.g. fractured, porous etc.). These findings support the hypothesis that the dimensionless SSTM is scale-independent, i.e., one value of σ^2 would be sufficient to characterise the dispersivity at different flow lengths. It is important to note that the role of the mean velocity in these calculations. We used 0.5 m/day to represent an indicative value in real aquifers, but the character of solutions do not change, if we assume a different value; only the specific values of σ^2 would be changed to represent a given flow situation.
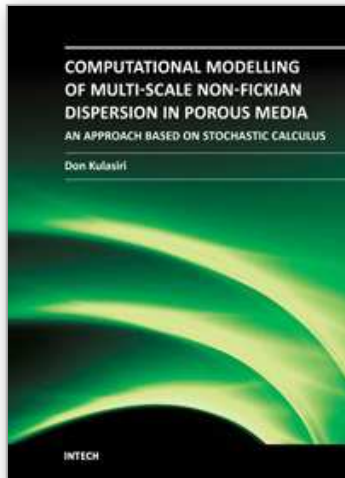
Computational Modelling of Multi-scale Solute Dispersion in Porous Media - An Approach Based on Stochastic Calculus
Edited by

This research monograph presents a mathematical approach based on stochastic calculus which tackles the "cutting edge" in porous media science and engineering - prediction of dispersivity from covariance of hydraulic conductivity (velocity). The problem is of extreme importance for tracer analysis, for enhanced recovery by injection of miscible gases, etc. This book explains a generalised mathematical model and effective numerical methods that may highly impact the stochastic porous media hydrodynamics. The book starts with a general overview of the problem of scale dependence of the dispersion coefficient in porous media. Then a review of pertinent topics of stochastic calculus that would be useful in the modeling in the subsequent chapters is succinctly presented. The development of a generalised stochastic solute transport model for any given velocity covariance without resorting to Fickian assumptions from laboratory scale to field scale is discussed in detail. The mathematical approaches presented here may be useful for many other problems related to chemical dispersion in porous media.

INTECH
open science | open minds